POLSKA AKADEMIA NAUK
INSTYTUT MASZYN PRZEPŁYWOWYCH

TRANSACTIONS OF THE INSTITUTE OF FLUID-FLOW MACHINERY

PRACE INSTYTUTU MASZYN PRZEPŁYWOWYCH

100

WYDAWNICTWO IMP PAN

GDAŃSK 1996

THE TRANSACTIONS OF THE INSTITUTE OF FLUID-FLOW MACHINERY

exist for the publication of theoretical and experimental investigations of all aspects of the mechanics and thermodynamics of fluid-flow with special reference to fluid-flow machines

*

PRACE INSTYTUTU MASZYN PRZEPŁYWOWYCH

poświęcone są publikacjom naukowym z zakresu teorii i badań doświadczalnych w dziedzinie mechaniki i termodynamiki przepływów, ze szczególnym uwzględnieniem problematyki maszyn przepływowych

Wydanie publikacji dofinansowane zostało przez PAN ze środków DOT uzyskanych z Komitetu Badań Naukowych

EDITORIAL OFFICE – REDAKCJA

Wydawnictwo Instytutu Maszyn Przepływowych
Polskiej Akademii Nauk
ul. Gen. Józefa Fiszera 14, 80-952 Gdańsk, skr. poczt. 621,
☎ (0-58) 46-08-81 wew. 141, fax: (0-58) 41-61-44,
e-mail: esli@imppan.imp.pg.gda.pl

ISSN 0079-3205

TRANSACTIONS OF THE INSTITUTE OF FLUID-FLOW MACHINERY

1996 Zeszyt 100

ANATOL JAWOREK[1]

Spherical probe for measuring charge on a single airborne particle

The probe developed consists of two concentric metal spheres, the inner of which is a collector and the outer serves as a shield. Two circular openings are made on opposite sides in the outer sphere. Through these openings an airborne particle can flow into the internal zone of the probe. The charged single particle induces a measuring signal on the inner electrode, before it is finally discharged after impacting on the electrode. The amplitude of the generated voltage signal depends almost uniquely on the particle charge. The method presented in the paper is capable of measuring the charge on aerosol particles down to $3 \cdot 10^{-14}$C with an accuracy of about ±5%.

1. Introduction

In many fields of electrostatic applications such as electrostatic precipitation, electrostatic printing or copying, electrodynamic spraying, and also in atmospheric research, it is necessary to measure the charge on a single macroscopic particle. Among the numerous methods for measuring charge on airborne particles, only inductive [1-7] and contact [8, 9] probes allow the measurement of charge *in situ* and in real time. The inductive probes are usually made in the form of a cylinder or ring, through which a particle flows without mechanical contact with the electrode, only inducing an electric potential on its surface. The contact probes are made in the form of a collector of arbitrary shape on which each particle is captured. The impacting particles are discharged generating an electrical signal in a measuring circuit.

Unlike contact probes the inductive probes do not remove the flowing particles, however they need to be calibrated [7]. Under certain conditions, the contact probes allow us to measure the absolute charge on a particle.

The inductive probes have been considered by many authors, for example by MacLatchy and Chipman [5], Weinheimer [6] and Jaworek [7]. A cylindrical contact probe has been described by Krupa and Jaworek [8, 9]. The alternative

[1]Institute of Fluid-Flow Machinery, Department of Plasma Dynamics, Fiszera 14, 80-952 Gdańsk

spherical probe has hitherto not been presented in the literature, except a short communication [10]. In the present paper the detailed characteristics of a spherical probe are considered.

The spherical probe consists of a spherical collector placed concentrically inside a spherical grounded metal shield, as shown schematically in Fig. 1. At diametrically opposite sides of the outer sphere two circular openings are made to allow the particles to enter the internal zone of the probe. It is assumed that a single particle enters through one of the openings and impacts on the internal sphere (collector). The flowing particle induces an electric charge on the collector. The charge induced on the collector is neutralized by that on the impacting particle after its collision with the collector. It results from the following theoretical considerations that the lower measurement limit of charge on a particle is about 10^{-13}C for the spherical probe.

The advantage of the spherical probe over the cylindrical probe is that there is only one kind of signal generated by the particles entering the probe, i. e. that generated by the particles impacting on the collector. When the diameter of the internal electrode (wire) of a cylindrical probe is too small or the particles are too fine, a number of the particles can flow by the collecting electrode, generating the induced signals only. In the spherical probes, the internal electrode is usually large, and the number of particles flowing by the sphere can be negligible.

The charge on a single impacting particle can be determined from the amplitude of the signal generated. The signals can be recorded by a storage oscilloscope or classified by a signal analyzer. The probe was successfully used in measuring the charge on droplets sprayed electrohydrodynamically.

The main measurement parameters such as time domain response, frequency response, sensitivity, charge limit etc. have been determined theoretically.

2. Time domain response

It is assumed that the two concentric spheres of the probe form a spherical condenser of regular shape, and that each particle entering the probe flows with a constant velocity along a straight line parallel to the axis joining the centres of the spheres and the openings (Fig. 1). The effect of the openings in the outer sphere on the charge induced on the collector is neglected in the following considerations. It is also assumed that a particle enters the probe at the moment of $t = 0$. The charge on the inner electrode induced by a charged particle (assumed to be a point charge) entering the probe is [11]:

$$Q_i = -Q \frac{a}{b-a} \frac{b-\rho}{\rho} \tag{1}$$

with the radial distance of the particle from the centre of the spheres ($\rho > a$):

$$\rho = \left\{ \left[(b^2 - l^2)^{1/2} - vt \right]^2 + l^2 \right\}^{1/2}, \tag{2}$$

where Q is the particle charge, l – the distance of the particle trajectory from the sphere center (impact parameter), v – the particle velocity, and a and b are the radii of the inner and outer electrodes, respectively (Fig. 1).

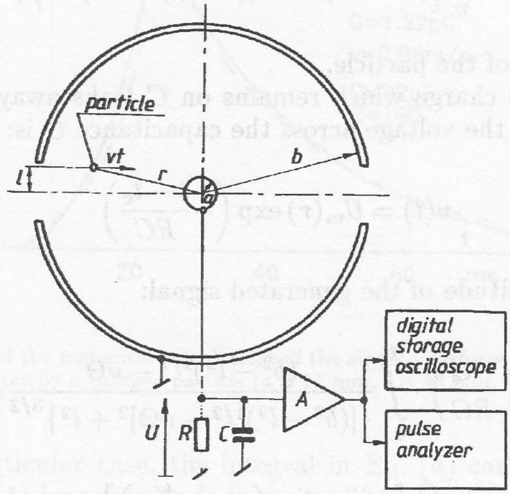

Fig. 1. Schematic diagram of the spherical probe and measuring circuit.

The charge induced by the particle before it reaches the entrance opening is assumed to be negligible.

The differential equation for the voltage $u(t)$ at the input of the measuring amplifier is:

$$\frac{dQ_i}{dt} = C\frac{du(t)}{dt} + \frac{u(t)}{R}, \tag{3}$$

where R, C are the resistance and capacitance at the input of the measuring circuit. The capacitance C is the sum of the probe capacitance, the input capacitance of the amplifier, the stray capacitance of the connecting wire and an additional discrete capacitor used to adjust the total capacitance to a required value. The resistance R is composed of the input (leakage) resistance of the amplifier and a discrete resistor connected parallelly.

The first term on the right hand side of Eq. (3) is the current charging the capacitance C while the second describes the current which leaks away via the resistance R.

The general solution of Eq. (3) is:

$$u(t) = \frac{-vQab}{C(b-a)} \exp\left(\frac{-t}{RC}\right) \cdot \int_0^t \frac{(b^2-l^2)^{1/2} - v\Theta}{\left(\left((b^2-l^2)^{1/2} - v\Theta\right)^2 + l^2\right)^{3/2}} exp\left(\frac{\Theta}{RC}\right) d\Theta, \tag{4}$$

with initial condition $u(t=0)=0$, and the condition that $a<(b^2-l^2)^{1/2}-vt\leq b$. At the time moment t_c the particle collides with the collector:

$$t_c=\frac{1}{v}\left\{(b^2-l^2)^{1/2}-[(a+r)^2-l^2]^{1/2}\right\}, \tag{5}$$

where r is the radius of the particle.

After collision the charge which remains on C leaks away exponentially via the resistance R, and the voltage across the capacitance C is:

$$u(t)=U_m(r)\exp\left(-\frac{t-t_c}{RC}\right) \tag{6}$$

where U_m is the amplitude of the generated signal:

$$U_m=\frac{Q}{C}\frac{vab}{b-a}\exp\left(\frac{-t_c}{RC}\right)\cdot\int\limits_0^{t_c}\frac{(b^2-l^2)^{1/2}-\nu\Theta}{\{[(b^2-l^2)^{1/2}-\nu\Theta]^2+l^2\}^{3/2}}exp\left(\frac{\Theta}{RC}\right)d\Theta+$$

$$+\frac{Q}{C}\left[1+\frac{a}{b-a}\left(1-\frac{b}{a+r}\right)\right]. \tag{7}$$

The first term in Eq. (7) results from Eq. (4) with time t_c given by Eq. (5), while the second one arises from the increment of charge on the capacitance C at the moment of collision $t=t_c$. The second term in Eq. (7) is derived with the assumption that the particle conductivity, γ, is high enough for the particle to be discharged in a negligible time period, compared to the time constant of the input circuit. In other words it is assumed that $\epsilon/\gamma\ll RC$, where ε is the particle permittivity. When the particle collides with the collector the charge on it is partially neutralized, and the resultant charge is added to that on the capacitance C. The drawings of the signal, obtained numerically, have been compared with oscilloscope recordings such as, for example, that shown in Fig. 2. The general conclusion is that the theoretical results are in good agreement with experiments.

The effect of various parameters on the signal waveform and its amplitude is presented in Fig. 3 and 4.

The waveform of the voltage signal generated by the probe is shown in the normalized form in Fig. 3a. The waveform only weakly changes with the impact parameter l/a.

As is shown in Fig. 4a, the amplitude of the signal only slightly decreases with the impact parameter if l/a is kept ≤ 0.5, for all values of the normalized time of particle flight b/vRC. For the values of $l/a>0.5$ (longer distances of the particle trajectory from the system axis), the amplitude of the generated signal decreases of a few percents as compared to $l/a=0$. However in practice, the inlet opening is smaller than the limiting value of the impact parameter, and in further theoretical considerations it is assumed that the impact parameter l/a is equal

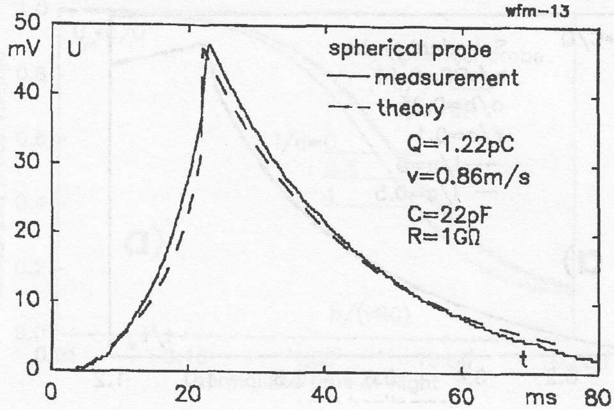

Fig. 2. Comparision of the numerical calculations of the signal waveform with an oscilloscope recording of a waveform generated by a charged particle (a = 11 mm, b = 44 mm, r = 1.6 mm).

to 0. In this particular case, the integral in Eq. (4) can be solved analytically. Integrating Eq. (4) by parts leads to a simplified solution of Eq. (3):

$$u(t) = \frac{-Qa}{C(b-a)}\frac{b}{vRC}\exp\left(\frac{b-vt}{vRC}\right)\left[Ei\left(\frac{-b}{vRC}\right) - Ei\left(\frac{vt-b}{vRC}\right)\right]$$
$$-\frac{Qa}{C(b-a)}\left[exp\left(\frac{-t}{RC}\right) - \frac{b}{b-vt}\right], \qquad (8)$$

where $Ei(.)$ denotes the exponential-integral function.

In this special case the amplitude of the measured signal equals the voltage across the capacitor C at the moment of collision:

$$U_m(r) = \frac{-Qa}{C(b-a)}\frac{b}{vRC}\exp\left(\frac{a+r}{vRC}\right)\left[Ei\left(\frac{-b}{vRC}\right) - Ei\left(\frac{a+r}{vRC}\right)\right] +$$
$$-\frac{Qa}{C(b-a)}\left[exp\left(-\frac{b-a-r}{vRC}\right) - \frac{b}{a+r}\right] + \frac{Q}{C}\left[1 + \frac{a}{b-a}\left(1 - \frac{b}{a+r}\right)\right]. \qquad (9)$$

The effect of the particle radius, r, on the signal waveform is presented in Fig. 3b. It can be seen from Fig. 3b that the shape of the waveform and also the signal amplitude only slightly change with the size of the particle. The signal amplitude increases with the increase in the particle diameter when the normalized time of particle flight b/vRC is greater than 1. Only for $b/vRC < 0.1$ the signal amplitude is practically independent of the relative particle radius normalized to the collector radius (Fig. 4b), and the approximate relation can be used with the accuracy better than 2%. In this case the amplitude (7) can be assumed to be

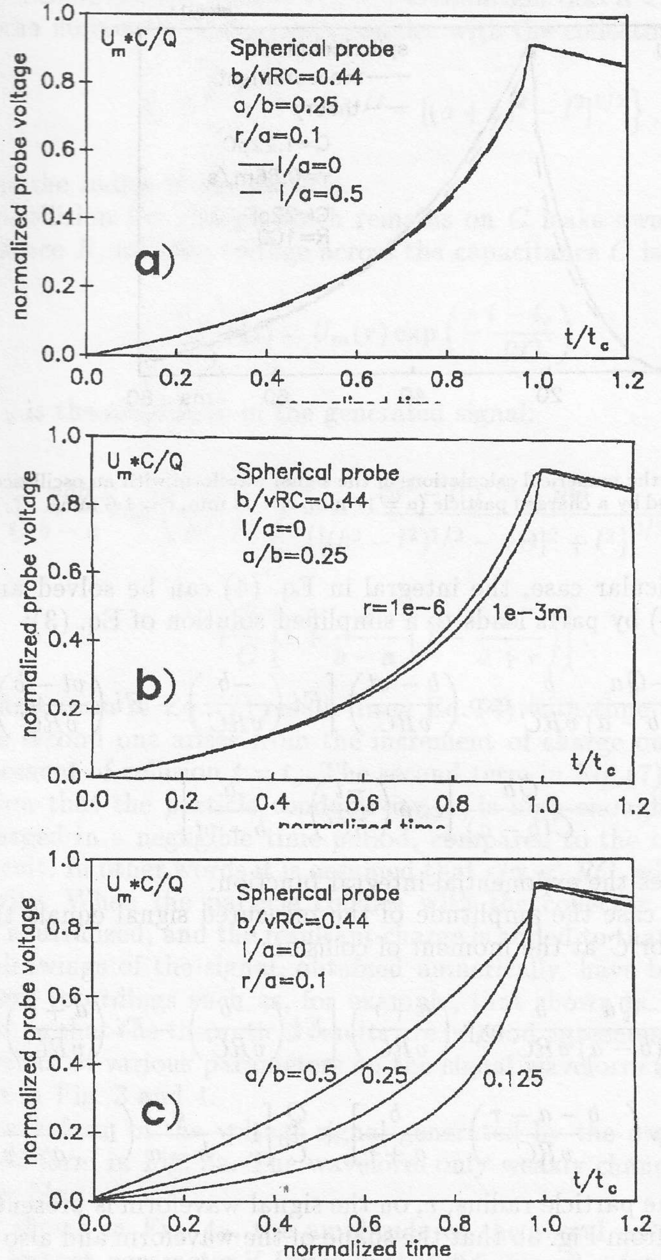

Fig. 3. Effect of the impact parameter l/a – (a), particle radius r/a – (b), collector radius a/b – (c), on the signal waveform.

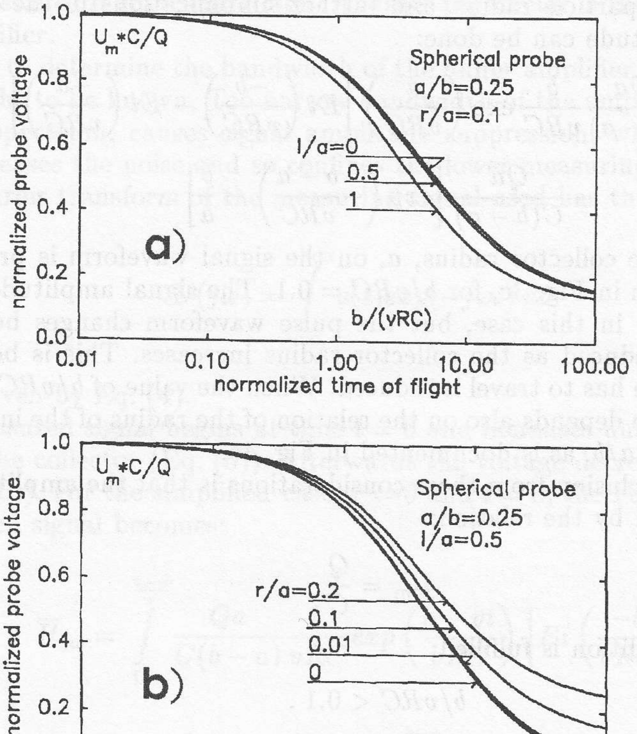

Fig. 4. Normalized signal amplitude versus normalized time of flight b/vRC of a charged particle for different values of the impact parameter l/a – (a), particle radius r/a – (b), collector radius a/b – (c).

independent of the particle radius, and further simplifications in the expression for the signal amplitude can be done:

$$U_m = \frac{-Qa}{C(b-a)}\frac{b}{vRC}\exp\left(\frac{a}{vRC}\right)\left[Ei\left(\frac{-b}{vRC}\right) - Ei\left(\frac{-a}{vRC}\right)\right] +$$
$$-\frac{Qa}{C(b-a)}\left[exp\left(-\frac{b-a}{vRC}\right) - \frac{b}{a}\right]. \qquad (10)$$

The effect of the collector radius, a, on the signal waveform is presented in the normalized form in Fig. 3c, for $b/vRC = 0.1$. The signal amplitude does not change significantly in this case, but the pulse waveform changes because the pulse duration is reduced as the collector radius increases. This is because the distance the particle has to travel is reduced. When the value of b/vRC increases, the signal amplitude depends also on the relation of the radius of the inner sphere to the outer sphere a/b, as is documented in Fig. 4c.

The general conclusion from these considerations is that the amplitude of the signal is determined by the relation:

$$U_m = \frac{Q}{C} \qquad (11)$$

if the following condition is fulfilled:

$$b/vRC < 0.1\,. \qquad (12)$$

In this case the signal amplitude is also independent of $l/a, r/a$ and b/vRC parameters.

The condition (12) is fulfilled if the velocity of the particle is high enough compared to the b/RC ratio. The physical meaning is that only a little of the charge induced on the collector can leak away before the particle collides with it. The time $(b-a)/v$, and then the required particle velocity can be estimated from oscilloscope recordings. The condition (12) is very useful in practice, but it is not necessary for measuring the particle charge properly. It requires a very high resistance R in the measuring circuit, and/or high particle velocity. When the condition (12) is difficult to fulfill, the charge can be determined from the measurements using Eqs.(9) or (10).

Usually R has to be greater than $10^9\Omega$, and $v > 1$ m/s. The increasing of the capacitance C is limited by a resulting reduction in the voltage induced. For example, for the probe and circuit used in the experiment, C=317 pF, $R = 10^9\Omega$ and $b = 0.022$ m, the particle velocity must be higher than 0.7 m/s, to overcome the reduction of the signal amplitude (see Fig. 4).

3. Frequency characteristics of the signal

In order to use the spherical probe correctly, the parameters of the measuring circuit have to be chosen properly. The capacitance C ought to be possibly small, and the resistance R sufficiently high. Another parameter is the bandwidth of the buffer amplifier.

In order to determine the bandwidth of the buffer amplifier the signal spectral density ought to be known. Too narrow bandwidth of the amplifier, compared to the signal spectrum, causes signal amplitude suppression, while too wide bandwidth increases the noise and so confines the lower measuring limit.

The Fourier transform of the measuring signal used has the form:

$$U(j\omega) = \int_{-\infty}^{+\infty} u(t) exp(-j\omega t)\, dt \tag{13}$$

with $u(t)$ given by Eq. (4).

The measured signal begins at time $t = 0$ and increases until the particle collides with the collector (Eq. (5)). Afterwards the voltage decreases exponentially (as in Eq. (6)). For the simplified case, $r = 0$ and $l = 0$, the Fourier transform of the measured signal becomes:

$$\overline{U}_{j\omega} = \int_0^{\frac{b-a}{v}} \frac{Qa}{C(b-a)} \frac{b}{vRC} exp\left(\frac{b-vt}{vRC}\right) \left[Ei\left(\frac{-b}{vRC}\right) \right.$$

$$\left. - Ei\left(\frac{vt-b}{vRC}\right)\right] exp(-j\omega t) dt + \int_0^{\frac{b-a}{v}} \frac{Qa}{C(b-a)} \left[exp\left(\frac{-t}{RC}\right) \right.$$

$$\left. - \frac{b}{b-vt}\right] exp(-j\omega t) dt - \int_{\frac{b-a}{v}}^{+\infty} U_m exp\left(\frac{b-a-vt}{vRC}\right) exp(-j\omega t) dt\,. \tag{14}$$

The absolute value of $\mid \overline{U}(j\omega) \mid$, which is the distribution of the intensity of the signal as a function of frequency, has been determined numerically, and is plotted in Fig. 5.

It is assumed that the transfer function of the amplifier has only one dominant pole, and the response of the amplifier to the excitation in the form of delta function $\delta(0)$ is:

$$h(t) = A_o \omega_o exp(-\omega_o t)\,. \tag{15}$$

where ω_o is the cut-off frequency of the amplifier and A_o is its *dc* voltage gain.

The convolution of two functions is given by the relation:

$$y(t) = \int_0^t u(t) h(t-\tau) d\tau\,. \tag{16}$$

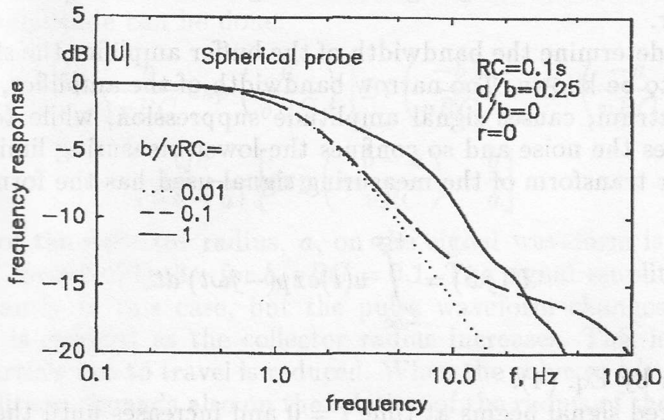

Fig. 5. Frequency response of the spherical probe.

For the impulse response of the amplifier (13) and the measured signal $u(t)$ given by Eq. (4) with $r = 0$ and $l = 0$, the amplifier output voltage for $t \leq (b-a)/v$ is:

$$y(t) = \frac{QA_o\omega_o a}{vC\left(1-\frac{a}{b}\right)} \int_0^t exp\left(\frac{-\tau}{RC}\right) exp[-\omega_o(t-\tau)] \int_0^\tau \frac{exp\left(\frac{\Theta}{RC}\right)}{\left(\frac{b}{v}-\Theta\right)^2} d\Theta\, d\tau \qquad (17)$$

and for $t > (b-a)/v$:

$$y(t) = \frac{QA_o\omega_o a}{vC\left(1-\frac{a}{b}\right)} \int_0^{\frac{b-a}{v}} exp\left(\frac{-\tau}{RC}\right) exp[-\omega_o(t-\tau)] \int_0^\tau \frac{exp\left(\frac{\Theta}{RC}\right)}{\left(\frac{b}{v}-\Theta\right)^2} d\Theta\, d\tau +$$

$$+A_o\omega_o U_m \int_{\frac{b-a}{v}}^t exp[-\omega_o(t-\tau)] exp\left(\frac{-\tau + (b-a)/v}{RC}\right) d\tau \qquad (18)$$

Eqs.(17) and (18) describe the signal waveform after passing the signal through the amplifier. At the input of the amplifier the pulse attains its maximum at time t_c given by (4), or when $l = r = 0$ given by $t_c = (b-a)/v$. However, at the output of the amplifier, the signal reaches its maximum value after a delay time Δt. The delay Δt can be determined by differentiating the equation (17) with respect to t, and setting the result to zero:

$$\frac{dy}{dt} = \frac{U_m\omega_o}{\omega_o RC - 1}\left\{-\frac{1}{\omega_o RC} exp\left(\frac{b-a-vt}{vRC}\right) + \right.$$

$$+(\omega_o RC-1)exp(-\omega_o t)\left[\frac{exp\left(\omega_o RC\frac{b-a}{vRC}\right)}{(\omega_o RC-1)}-\frac{U_i}{U_m}\right]\Bigg\} \tag{19}$$

where:

$$U_i=\frac{QA_o\omega_o a}{vC\left(1-\frac{a}{b}\right)}\int\limits_0^{\frac{b-a}{v}} exp\left(\frac{-\tau}{RC}\right)exp(\omega_o\tau)\int\limits_0^{\tau}\frac{exp\left(\frac{\Theta}{RC}\right)}{\left(\frac{b}{v}-\Theta\right)^2}d\Theta\, d\tau\,, \tag{20}$$

is the voltage at the amplifier output, at the moment of impact. After that the voltage decays exponentially according to Eq. (6). From Eq. (19) one obtains:

$$t_m=\frac{RC}{\omega_o RC-1}ln\left\{(\omega_o RC-1)\omega_o RC\; exp(-\omega_o t)\left[\frac{exp\left(\omega_o RC\frac{b-a}{vRC}\right)}{(\omega_o RC-1)}-\frac{U_i}{U_m}\right]\right\}. \tag{21}$$

In most practical cases the second term U_i/U_m in equation (21) is of the order of magnitude of 1 and can be omitted in comparison to the first term which usually is much greater than 1. Then, the delay approximately equals

$$\Delta t=\frac{RC\; ln(\omega_o RC)}{\omega_o RC-1}. \tag{22}$$

The delay time Δt is plotted in Fig. 6 in the normalized form as a function of the amplifier bandwidth Δf defined as $\Delta f=\omega_o/2\pi$.

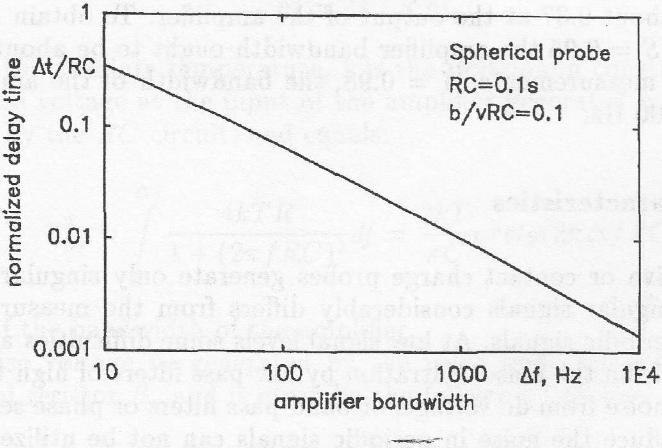

Fig. 6. Delay time of the signal normalized amplitude.

The signal amplitude attenuation S due to the amplifier bandwidth, defined as the ratio of the amplitude $U_o(i.e.y(t)$ at time $t=\Delta t)$ of the signal at the output of the amplifier to the $A_o U_m$ is:

$$S = \frac{U_o}{A_o U_m} = \frac{U_i}{U_m} \exp\left(-\omega_o RC \frac{ln(\omega_o RC)}{\omega_o RC - 1}\right) exp\left(-\omega_o \frac{b-a}{v}\right) +$$

$$+ \frac{\omega_o RC}{\omega_o RC - 1}\left[exp\left(\frac{-ln(\omega_o RC)}{\omega_o RC - 1}\right) - exp\left(\omega_o RC \frac{-ln(\omega_o RC)}{\omega_o RC - 1}\right)\right]. \quad (23)$$

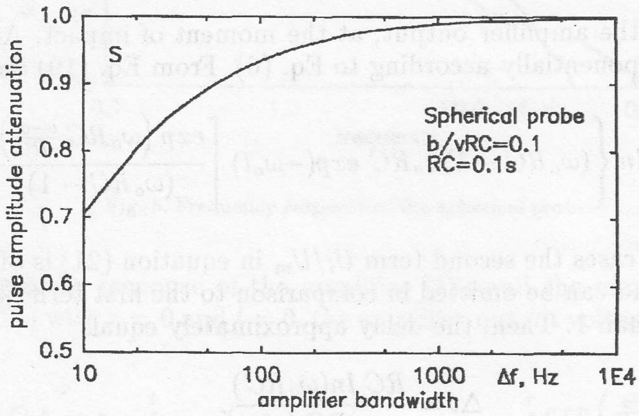

Fig. 7. Pulse amplitude attenuation at the output of the amplifier with the bandwidth Δf.

As it is seen from Fig. 7, if the bandwidth of the amplifier ($\omega_o/2\pi$) equals the bandwidth of the signal spectrum ($1/2\pi RC$), the normalized signal amplitude, S, is reduced to about 0.37 at the output of the amplifier. To obtain an amplitude attenuation of $S = 0.95$ the amplifier bandwidth ought to be about 100 Hz. For more accurate measurements, $S = 0.98$, the bandwidth of the amplifier should rise to about 300 Hz.

4. Noise characteristics

The inductive or contact charge probes generate only singular signals. The detection of singular signals considerably differs from the measurements of dc voltages and periodic signals. At low signal levels some difficulties arise in distinguishing them from the noise. Filtration by low-pass filters of high time constant to remove the noise from dc voltage, or band-pass filters or phase sensitive detectors used to reduce the noise in periodic signals can not be utilized in the case of a singular signal detection. The noise characteristics of the measuring circuit need therefore special attention.

The lower limit in the measurement of the particle charge is mainly confined by noise. In this section only the thermal noise generated by the input resistance

R, and equivalent noise generated by a measuring electrometer valve amplifier will be considered. These considerations predict a lower theoretical limit of the charge that can be measured by the spherical probe. The noise caused by electromagnetic fields is not taken into considerations because they can be easily removed by shield and grounding. Also the flicker noise of the resistors within the circuit are excluded from the calculations.

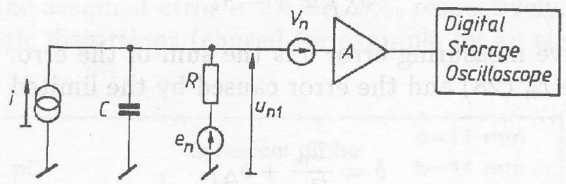

Fig. 8. Equivalent circuit of the spherical probe with noise sources.

The schematic diagram of the measurement circuit with an electrometer valve amplifier, including the equivalent noise generators is presented in Fig. 8. The source of the measured signal is represented by a current generator i. A voltage generator e_n is the source of the thermally generated noise by the resistor R. The noise generated by an valve amplifier is represented by the equivalent source v_n in series with the input of an ideal amplifier [12].

The rms voltage of the noise generated by a resistor of resistance R in the frequency bandwidth df is given by the following equation:

$$\overline{e}_n^2 = 4kTR\, df, \tag{24}$$

where T is the absolute temperature, k is the Boltzmann constant.

The noise voltage at the input of the amplifier generated by the source $\overline{e}_n^2$ is attenuated by the RC circuit, and equals:

$$\overline{u}_{n1}^2 = \int_0^{\Delta f} \frac{4kTR}{1+(2\pi fRC)^2} df = \frac{2kT}{\pi C} arctg(2\pi \Delta f RC), \tag{25}$$

where Δf if the bandwidth of the amplifier.

The noise voltage v_n generated by the valve amplifier is represented by a hypothetical resistor R_v and is given by the following relation:

$$\overline{v}_n^2(f) = 4kTR_v\, df. \tag{26}$$

The effective rms value of the input noise voltage is:

$$\overline{u}_n^2 = \overline{u}_{n1}^2 + \overline{v}_n^2. \tag{27}$$

The relative measuring uncertainty due to noise is defined as the rms of the effective noise voltage related to the maximum value of the measured signal U_m:

$$\delta_n = \frac{\overline{u}_n}{U_m}. \tag{28}$$

The error caused by the bandwidth of the amplifier due to suppression of the signal amplitude is:

$$\delta_{\Delta f} = 1 - S. \tag{29}$$

The total relative measuring error δ is the sum of the error corresponding to the generated noise δ_n (28) and the error caused by the limited bandwidth of the amplifier $\delta_{\Delta f}$ (29):

$$\delta = \frac{\overline{u}_n}{U_m} + \delta_{\Delta f}. \tag{30}$$

In Eq. (30) the voltage U_m can be assumed to be the lowest signal amplitude measured with the total error δ. The value of the minimum charge $Q_{\min}$ measured with the error δ (the lower measuring limit) is:

$$Q_{\min}(\Delta f) = C \frac{\overline{u}_n}{\delta - \delta_{\Delta f}} \tag{31}$$

and is plotted in Fig. 9 as the function of the bandwidth of the amplifier, and for different errors δ.

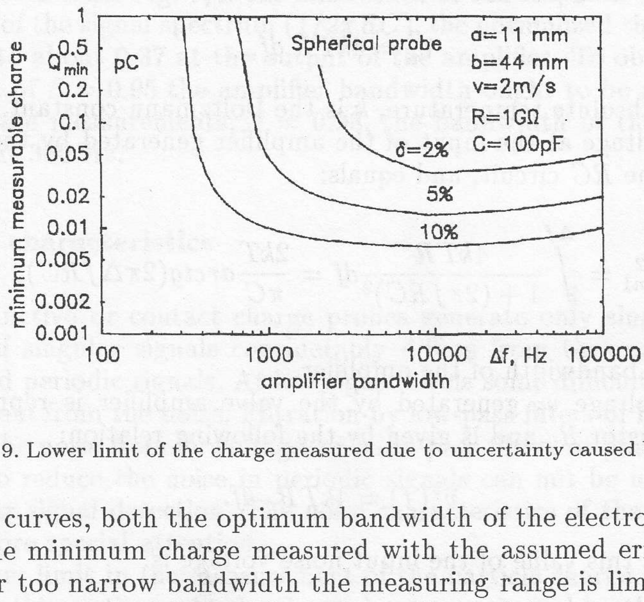

Fig. 9. Lower limit of the charge measured due to uncertainty caused by noise.

From the curves, both the optimum bandwidth of the electrometer valve amplifier and the minimum charge measured with the assumed error δ can be determined. For too narrow bandwidth the measuring range is limited by the suppression error. For wider bandwidth the lower limit of the measurement increases because of the decrease in the signal-to-noise ratio. This is conspicuous particularly for lower values of the input resistance R, because the thermally generated noise is not attenuated by the RC circuit. The effect of the input capacitance on the measuring range is shown in Fig. 10. With the increase in the input capacitance the lower measuring limit increases because the induced charge is lower, regardless of the attenuation of the noise generated by the resistor R.

For the input capacity $C = 100$ pF, and input resistance $R = 1$ GΩ, the minimum charge which can be measured by the spherical probe is for example 0.05 pC or 0.01 pC if the assumed error is 2% or 10%, respectively.

The electromagnetic distortions (caused for example by an electrical discharge)

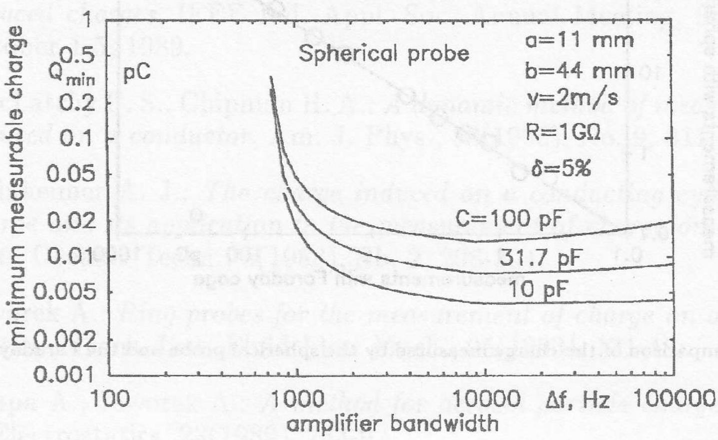

Fig. 10. The effect of input capacitance C on the lower measuring limit for the spherical probe.

or line interference (50 Hz) can cause the lower measuring limit to increase even by an order of magnitude.

5. Experiment

The charges of test particles measured by means of the spherical probe were compared with the results obtained using a Faraday cage as a reference method.

Droplets of distilled water generated electrohydrodynamically from a metal capillary connected to a dc voltage source were used as test particles. The dripping pressure was kept constant by maintaining the water at a fixed level. The mean radius of the droplets ranged from 1.6 mm down to 0.5 mm, whereas the dripping frequency varied from 1 to about 20 Hz, depending on the voltage applied. The particle charges were measured alternately with the Faraday cage and the spherical probe, keeping the dripping and charging conditions constant. A sensitive electrometer was used to measure the charge on the Faraday cage. The results obtained from recording the series of signals from individual droplets of the same size are plotted in Fig. 11. Each point on the plot is the average result of measuring the charge on approximately 100 droplets. The relation appears to be linear over the tested range of charge. The discrepancy between the data is within the uncertainty of the measurements. For charges greater than 10^{-12} C the relative difference of the results obtained by the two methods is $< \pm 5\%$, and for charges $< 10^{-12}$ C it is about 10%.

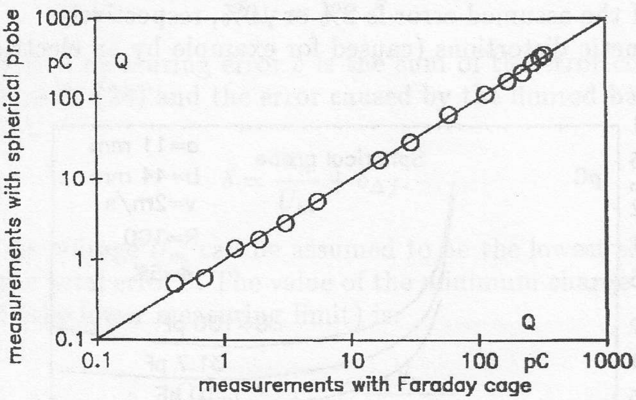

Fig. 11. Comparison of the charge measured by the spherical probe and the Faraday cage.

6. Conclusions

Theoretical and experimental investigations of the measurement performance of the spherical probe lead to the following conclusions:

1. The probe allows the measurement of the charge on droplets or particles down to $3 \cdot 10^{-14}$ C with an error lower than 5%. The lower charge measurement limit is determined by the thermal noise associated with the input resistance of the measuring circuit and measuring amplifier.

2. There is only little influence of the particle velocity, its radius and the impact parameter upon the signal amplitude and the measured results, if the condition $b/vRC < 0.1$ is satisfied. This condition requires high input resistance of the measuring circuit and particle velocities of a few m/s.

3. If the condition $b/vRC < 0.1$ is difficult to fulfill, the charge can also be determined, but it must be calculated from the voltage measured using Eqs. (9) or (10).

Manuscript received in February 1995

References

[1] Hendricks Ch. D., Yeung K. F.: *Technique of single particle charge measurement*, IEEE Trans. Ind. Appl., 12(1976), No. 1, 56-63.

[2] Gajewski J. B.: *Charge measurement of dust particle in motion*, J. Electrostatics, 15(1984), 67-79.

[3] Williams T. J., Wilmshurst T. H., Bailey A. G.: *An in flight particle charge detector*, 7th Int. Conf. Electrostatic Phenomena, Oxford April 8-10, 1987.

[4] Rossner M., Singer H.: *Measurement of micrometer particles by means of induced charges*, IEEE Ind. Appl. Soc. Annual Meeting, San Diego, USA, October 1-5, 1989.

[5] MacLatchy C. S., Chipman H. A.: *A dynamic method of measuring the charge induced on a conductor*, Am. J. Phys., 58(1990), No. 9, 811-6.

[6] Weinheimer A. J.: *The charge induced on a conducting cylinder by a point charge and its application to the measurement of charge on precipitation*, J. Atm. Oceanic Techn., 5(1988), No. 2, 298-304.

[7] Jaworek A.: *Ring probes for the measurement of charge on a single airborne particle*, Trans. Inst. Fluid Flow Mach., 95(1993), 131-46.

[8] Krupa A., Jaworek A.: *A method for aerosol particle charge measurements*, J. Electrostatics, 23(1989), 283-92.

[9] Jaworek A., Krupa A.: *Charge detector for airborne particles*, J. Electrostatics, 25(1990), 185-99.

[10] Jaworek A., Krupa A.: *Sphere probe measuring charge on charged droplets or dust particles*, Pomiary, Automatyka, Kontrola, 38(1992), No. 9, 201-3, (in Polish).

[11] Smythe W. R.: *Static and dynamic electricity*, McGraw-Hill Book Company 1968.

[12] Hennel J.: *Lampy elektronowe*, WNT, Warszawa 1966.